Available online at www.sciencedirect.com

SciVerse ScienceDirect

Geochimica et Cosmochimica Acta 87 (2012) 21–34

Geochimica et Cosmochimica Acta

www.elsevier.com/locate/gca

Resilience of cold-water scleractinian corals to ocean acidification: Boron isotopic systematics of pH and saturation state up-regulation

Malcolm McCulloch [a,b,*], Julie Trotter [a], Paolo Montagna [c,d,e], Jim Falter [a,b], Robert Dunbar [f], André Freiwald [g], Günter Försterra [h], Matthias López Correa [i], Cornelia Maier [j], Andres Rüggeberg [k], Marco Taviani [e,l]

[a] *The UWA Oceans Institute and School of Earth and Environment, The University of Western Australia, Crawley 6009, Western Australia, Australia*

[b] *ARC Centre of Excellence in Coral Reef Studies, The University of Western Australia, Crawley 6009, Western Australia, Australia*

[c] *Lamont-Doherty Earth Observatory of Columbia University, 61 Route 9W, Palisades, NY 10964, USA*

[d] *Laboratoire des Sciences du Climat et de l'Environnement, Av. de la Terrasse, 91198 Gif-sur-Yvette, France*

[e] *ISMAR-CNR, via Gobetti 101, I-40129 Bologna, Italy*

[f] *Environmental Earth System Science, School of Earth Sciences, Stanford University, Stanford, CA 94305-4216, USA*

[g] *Senckenberg am Meer, Abteilung Meeresgeologie, Südstrand 40, D-26382 Wilhelmshaven, Germany*

[h] *Pontificia Universidad Católica de Valparaíso, Avda. Brazil 2950, Valparaíso, Chile and Huinay Scientific Field Station, Casilla 1150, Puerto Montt, Chile*

[i] *GeoZentrum Nordbayern, Universität Erlangen-Nürnberg, Loewenichstr. 28, D-91054 Erlangen, Germany*

[j] *Microbial Ecology and Biogeochemistry Group Laboratoire d'Océanographie de Villefranche-sur-Mer, BP 28, 06234 Villefranche-sur-Mer, France*

[k] *Renard Centre of Marine Geology (RCMG), Dept. of Geology and Soil Science, Ghent University, Krijgslaan 281, S8, B-9000 Gent, Belgium*

[l] *Biology Department, Woods Hole Oceanographic Institution, 266 Woods Hole Road, Woods Hole, MA 02543, USA*

Received 8 August 2011; accepted in revised form 19 March 2012; available online 27 March 2012

Abstract

The boron isotope systematics has been determined for azooxanthellate scleractinian corals from a wide range of both deep-sea and shallow-water environments. The aragonitic coral species, *Caryophyllia smithii*, *Desmophyllum dianthus*, *Enallopsammia rostrata*, *Lophelia pertusa*, and *Madrepora oculata*, are all found to have relatively high $\delta^{11}B$ compositions ranging from 23.2‰ to 28.7‰. These values lie substantially above the pH-dependent inorganic seawater borate equilibrium curve, indicative of strong up-regulation of pH of the internal calcifying fluid (pH_{cf}), being elevated by ~0.6–0.8 units (ΔpH) relative to ambient seawater. In contrast, the deep-sea calcitic coral *Corallium* sp. has a significantly lower $\delta^{11}B$ composition of 15.5‰, with a corresponding lower ΔpH value of ~0.3 units, reflecting the importance of mineralogical control on biological pH up-regulation.

The solitary coral *D. dianthus* was sampled over a wide range of seawater pH_T and shows an approximate linear correlation with $\Delta pH_{Desmo} = 6.43 - 0.71pH_T$ ($r^2 = 0.79$). An improved correlation is however found with the closely related parameter of seawater aragonite saturation state, where $\Delta pH_{Desmo} = 1.09 - 0.14\Omega_{arag}$ ($r^2 = 0.95$), indicating the important control that carbonate saturation state has on calcification. The ability to up-regulate internal pH_{cf}, and consequently Ω_{cf}, of the calcifying fluid is therefore a process present in both azooxanthellate and zooxanthellate aragonitic corals, and is attributed to the action of Ca^{2+}-ATPase in modulating the proton gradient between seawater and the site of calcification. These findings also show

* Corresponding author at: The UWA Oceans Institute and School of Earth and Environment, The University of Western Australia, Crawley 6009, Western Australia, Australia.

E-mail address: Malcolm.McCulloch@uwa.edu.au (M. McCulloch).

http://dx.doi.org/10.1016/j.gca.2012.03.027

that the boron isotopic compositions ($\delta^{11}B_{carb}$) of aragonitic corals are highly systematic and consistent with direct uptake of the borate species within the biologically controlled extracellular calcifying medium.

We also show that the relatively strong up-regulation of pH and consequent elevation of the internal carbonate saturation state (Ω_{cf} ~8.5 to ~13) at the site of calcification by cold-water corals, facilitates calcification at or in some cases below the aragonite saturation horizon, providing a greater ability to adapt to the already low and now decreasing carbonate ion concentrations. Although providing greater resilience to the effects of ocean acidification and enhancing rates of calcification with increasing temperature, the process of internal pH_{cf} up-regulation has an associated energetic cost, and therefore growth-rate cost, of ~10% per 0.1 pH unit decrease in seawater pH_T. Furthermore, as the aragonite saturation horizon shoals with rapidly increasing pCO_2 and $\Omega_{arag} < 1$, increased dissolution of the exposed skeleton will ultimately limit their survival in the deep oceans.

1. INTRODUCTION

Azooxanthellate cold-water scleractinian corals inhabit a diverse range of environments from deep-sea canyons and seamounts to the relatively shallow but cold-water environments found in high latitudes fjords. Despite their apparent isolation, they are vulnerable to environmental issues that also threaten shallow-water zooxanthellate corals of tropical reef systems. These incorporate both local disturbances (e.g. deep-sea trawling and deep ocean resource development) and the all-pervasive effects of global warming and ocean acidification (Roberts et al., 2006). Ocean acidification, the phenomenon of decreasing seawater pH and carbonate ion concentrations (Caldeira and Wickett, 2003), is of particular concern given that anthropogenically generated CO_2 is being injected into the sub-surface ocean (Orr et al., 2005) thereby driving these changes in seawater chemistry. For cold-water corals, which are already living at low levels of carbonate saturation (Thresher et al., 2011), the shoaling of the saturation horizon as carbonate saturation states decrease has the potential to cause dramatic declines in rates of calcification (Langdon and Atkinson, 2005; Kleypas et al., 2006; Turley et al., 2007), or the dissolution of the carbonate skeletons of those living at or close to the saturation horizon (Guinotte et al., 2006; Fautin et al., 2009; Thresher et al., 2011; Form and Riebesell, 2012). This suggests that they may have evolved adaptive strategies to counter the effects of low carbonate saturation states along with the cold-water conditions of the deep oceans. Understanding these longer-term evolutionary characteristics may therefore provide new critical information on the effects of ocean acidification on deep-sea ecosystems, as well as other calcifiers in general.

Scleractinian corals precipitate their calcium carbonate skeleton from an extracellular calcifying medium (Allemand et al., 2004) located at the interface between the coral polyp's basal cell layer and the underlying skeleton (Fig. 1). Although this is a strongly biologically mediated region (Al-Horani et al., 2003; Allemand et al., 2004), the process of aragonite precipitation is nevertheless still ultimately determined by the composition and conditions of the crystallising medium (Cohen and McConnaughey, 2003). Biological manipulation of pH at the site of calcification occurs by Ca^{2+}-ATPase pumping of Ca ions into the calcifying region in exchange for protons (Cohen and McConnaughey, 2003; Allemand et al., 2004). This process shifts the equilibrium composition of dissolved inorganic carbon (DIC) in favour of CO_3^{2-} relative to HCO_3^-, thus increasing the saturation state of the calcifying fluid (Ω_{cf}) upon which calcification is dependent. Increasing the carbonate saturation state at the site of calcification also has the potential to counter the effects of reduced carbonate saturation in seawater (Cohen and Holcomb, 2009; Holcomb et al., 2009). For example, the presence of cold-water corals near the aragonite saturation horizon (Fautin et al., 2009; Thresher et al., 2011) is consistent with both short (Maier et al., 2009; Form and Riebesell, 2012) and longer-term (Form and Riebesell, 2012) incubation experiments showing positive net calcification of *Lophelia pertusa* with an aragonite saturation state of less than one ($\Omega_{arag} < 1$). The absence of light harvesting symbiotic dinoflagellates in cold-water corals also avoids the complexities common to zooxanthellate organisms, where light enhanced calcification (Gattuso et al., 1999; Allemand et al., 2004) and the detrimental effects of bleaching can be problematic. Thus, determining the processes controlling both the internal, biologically mediated pH_{cf}, and hence the carbonate saturation state Ω_{cf} at the site of calcification, is likely to be key to understanding how biogenic calcifiers will respond to ocean acidification, in both cold deep waters as well as tropical reef environments.

Here we extend the novel approach taken by Trotter et al. (2011), based on boron isotopic systematics, to determine the relationship between seawater pH and the internal (extracellular) pH_{cf} at the site of calcification for azooxanthellate cold-water scleractinian corals. In biogenic carbonates, boron isotope variations (Vengosh et al., 1989; Hemming and Hanson, 1992) provide a measure of the pH of the calcifying medium due to the pH-dependent and isotopically distinctive speciation reaction between the borate ion, $B(OH)_4^-$, and boric acid, $B(OH)_3$ (Fig. 2). In contrast to earlier studies of cold-water corals (Blamart et al., 2007; Rollion-Bard et al., 2011), we find that the boron isotopic compositions ($\delta^{11}B_{carb}$) of scleractinian corals is generally highly systematic (Trotter et al., 2011) and consistent with direct uptake of the borate species within the biologically controlled extracellular calcifying medium. With proper species-dependent calibrations we show that this validates the use of boron isotope systematics as a pH proxy, which can be further applied to retrieve long-term records from both tropical (Pelejero et al., 2005; Wei et al., 2009) and cold water corals.

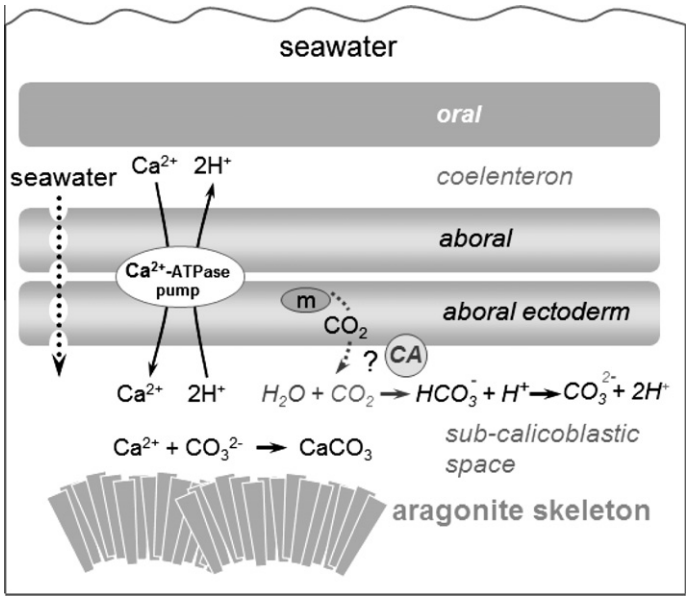

Fig. 1. Schematic of the calcification process in azooxanthellate cold-water corals (modified from Allemand et al., 2004). Removal of protons from the calcification site occurs primarily via Ca^{2+}-ATPase exchangers that pump $2H^+$ ions from the calcifying medium into the coelenteron in exchange for each Ca^{2+} ions. The carbonic anhydrases (CA) catalyse the forward reactions converting seawater derived HCO_3^- into CO_3^{2-} ions (Moya et al., 2008), the latter being essential for calcification. Due to the greater pH_{cf} in azooxanthallate corals (see discussion), it is likely that diffusion of CO_2 into the sub-calicoblastic space is minimal and thus the DIC of the calcifying fluid is similar to that in seawater (Erez, 2003).

2. SAMPLES AND METHODS

2.1. Coral collection

Both colonial and solitary cold-water scleractinian corals were collected live from a large range of depths and geographically disparate sites (Suppl. 1 on-line data). Samples were collected by submersibles, ROVs, dredge hauls, and SCUBA diving. *Desmophyllum dianthus* was collected live offshore southeast Australia by ROV (Jason) at 1050 m depth; by SCUBA at ~30 m in the cold shallow waters of the Comau Fjord, Chile (Försterra et al., 2005); and a large modern but dead specimen was collected by ROV (Nautile) at 932 m from the semi-enclosed Marmara Sea (Taviani et al., 2011), which separates the Black Sea from the Aegean Sea. Living samples of *D. dianthus*, *Caryophyllia smithii*, *Madrepora oculata*, and *L. pertusa* were dredged from 250 to 850 m at a number of sites in the Mediterranean Sea. Live *L. pertusa* was also collected by submersible (JAGO), ROV (QUEST), and dredged from 250 to 880 m at several sites in the northeast Atlantic Ocean. Two morphotypes of *Enallopsammia rostrata*, a robust (534 m) and delicate (1108 m) form, as well as a calcitic gorgonian *Corallium* sp. (942 m) were collected live by a manned submersible (PISCES V) off the NW Hawaiian Islands within the Pacific Ocean.

2.2. Seawater collection and measurements

The boron isotope pH proxy has been calibrated using measurements of seawater temperature, salinity, pH or the total alkalinity (TA), and dissolved inorganic carbon (DIC), to calculate seawater pH and the aragonite saturation state. All seawater pH values are reported using the "Total" pH scale and hence given the standard notation of pH_T (e.g. Marion et al., 2011). Reproducibility was typically ±0.01 units for pH_T measurements. Where possible, these parameters were determined for bottom waters collected at the coral sample sites. For samples where ambient seawater measurements are unavailable, data were sourced from the publically accessible GLODAP and CARINA ocean databases (cdiac.ornl.gov/oceans/) and calculated using CO2SYS Matlab version 1.1 (Lewis and Wallace, 1998) to ensure consistency (Table 1). It is important to acknowledge that these databases only provide an approximation of seawater pH, so are used cautiously as they may not correctly reflect the actual ambient conditions in which the corals calcified. Given that cold-water corals are distributed over a wide range of environments, it is also important to calculate carbonate system dissociation constants with the relevant seawater parameters, as these corrections (e.g. temperature, pressure) can be significant. Furthermore, seawater pH measurements are conventionally reported in databases at 25 °C, so it is necessary to correct these values to the much colder ambient seawater temperatures.

For DIC and TA, 3 × 500 ml seawater was sampled using Niskin bottles. Seawater was poisoned with 100 µl saturated mercury chloride ($HgCl_2$), and samples were stored at 10 °C until analysed. Analysis of DIC and TA of 500-ml samples was conducted at the University of Paris (http://soon.ipsl.jussieu.fr/SNAPOCO2/) and the CSIRO laboratories in Hobart following standard methods (Dickson et al., 2007). Reproducibility of the Dickson standard

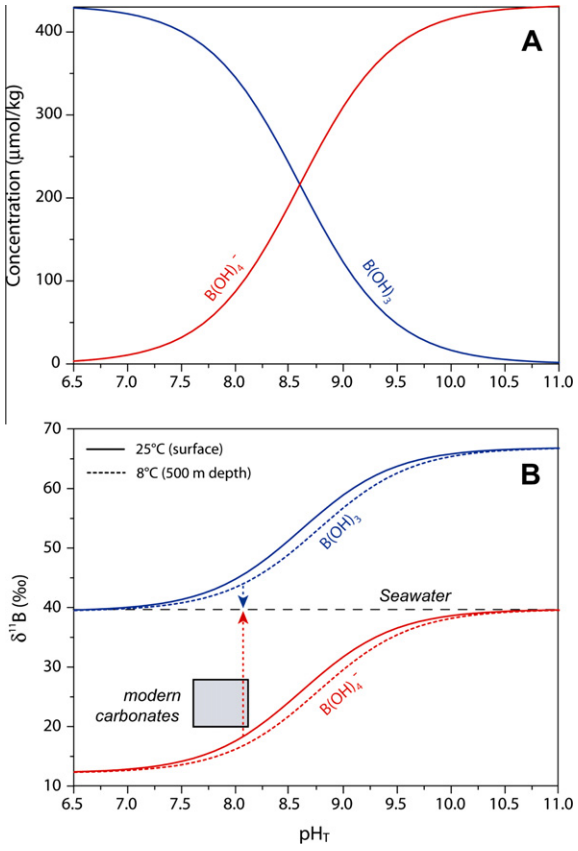

Fig. 2. (A) Boron speciation in seawater as a function of seawater pH_T (Total scale). (B) Boron isotope fractionation of ~27‰ between the boric and borate species (Klochko et al., 2006). Calcifiers appear to take up the borate ion $[B(OH)_4^-]$ exclusively and thus generally lie on or near the red borate curve. The blue and red arrows show the relative contribution of each species to the overall seawater $\delta^{11}B$ composition of 39.6‰. Grey box shows the typical $\delta^{11}B$ compositions of marine carbonates, which generally lie above the borate curve. (For interpretation of the references to colour in this figure legend, the reader is referred to the web version of this article.)

was ~3 µmol kg^{-1} for TA and ~2.8 µmol kg^{-1} for DIC, which are within the fixed tolerance limits. Direct seawater pH determinations reported from the Marnaut cruise (*D. dianthus*, Marmara Sea) were converted from NBS Scale to the pH_T Total Scale (Marion et al., 2011) and corrected from 25 °C to the *in situ* temperature and pressure at the coral sample site (Rae et al., 2011).

2.3. Boron isotope methods and systematics

Coral subsampling targeted the homogeneous fibrous skeletal portions from the corallum wall, avoiding centres of calcification where possible. Preparation, chemical processing, and mass spectrometry followed a variant of the di-caesium metaborate ($Cs_2BO_2^+$) PTIMS technique (Trotter et al., 2011). Briefly, the samples (20 mg) were pre-treated with 30% H_2O_2 to remove organic matter and the boron separated using cation and boron specific ion exchange chromatography. CsCl and mannitol were added to the B eluent then evaporated (<60 °C) under infrared light. After removal of organics using H_2O_2, the sample was digested in HCl, loaded directly onto the Ta filaments in a graphite suspension, then heated slowly to dryness under a ceramic heat lamp. A modern carbonate coral (NEP) was used as an in-house secondary standard to monitor the robustness and analytical reproducibility of the chemical process. The samples were analysed on a Thermo Scientific TRITON multi-collector thermal ionization mass spectrometer at the Research School of Earth Sciences at the Australian National University. The internal precision (2 s.d.) is 0.05% with a mean of 26.5‰ ($n = 30$) based on direct loads of the SRM951, and 0.08% ($n = 14$) based on the NEP in-house coral standard with the latter including chemical processing. Analysis of a single calcitic coral (*Corallium* sp.) was undertaken in duplicate using NTIMS due to its low boron concentration, following standard protocols (Vengosh et al., 1989; Hemming and Hanson, 1992; Pelejero et al., 2005).

The boron isotope variations are expressed in the conventional delta notation relative to NIST 951 standard as:

$$\delta^{11}B_{carb} = \left[\left({}^{11}B/{}^{10}B_{sample}\right)/\left({}^{11}B/{}^{10}B_{NIST951}\right) - 1\right] \times 1000 \quad (1)$$

The general principles behind the use of boron as a proxy for pH (Vengosh et al., 1991) are shown in Fig. 2. In seawater, boron exists as both trigonal boric acid $[B(OH)_3]$ and the tetrahedrally co-ordinated borate $[B(OH)_4^-]$ ion, with a pronounced isotope fractionation between the species of ~27‰. The fractionation factor is given by:

$$\alpha_{(B3-B4)} = \left[{}^{11}B/{}^{10}B_{B(OH)3}\right]/\left[{}^{11}B/{}^{10}B_{B(OH)4^-}\right] \quad (2)$$

Until recently, there has been some controversy regarding the most appropriate value of $\alpha_{(B3-B4)}$. However, direct determination by chemical equilibrium measurements of artificial seawater (Klochko et al., 2006), theoretical calculations (Zeebe, 2005; Rustad et al., 2010), $\delta^{11}B_{carb}$ measurements on some foraminifera (Foster, 2008; Rae et al., 2011) as well as recent reinterpretations of boron isotope systematics (Trotter et al., 2011), are now all generally consistent with a value of $\alpha_{(B3-B4)}$ between 1.026 of 1.028 rather than the previous value of 1.0194 (Kakihana et al., 1977). Accordingly, we use the experimental calibration of the boric/borate isotopic fractionation factor of 1.0272 (Klochko et al., 2006) for which temperature and salinity corrections appears to be relatively minor. However, we caution that experimental data is only available for the temperature range of 25–40 °C.

The other key assumption in the application of the boron isotope proxy for seawater pH is that only the tetrahedrally co-ordinated borate $B(OH)_4^-$ species is incorporated into the skeletons of biogenic calcifiers. This is important because the $\delta^{11}B_{carb}$ composition is assumed to be only that of the borate species. This suggests that the borate ion may be directly incorporated into the aragonite coral structure maintaining its tetrahedral coordination (Sen et al., 1994) via a reaction of the type (Trotter et al., 2011):

$$Ca^{2+} + 2B(OH)_4^- \rightarrow Ca(H_3BO_4) + B(OH)_3 + H_2O \quad (3)$$

Table 1
Coral species and depths with measured or sourced seawater parameters used for calibrating the δ^{11}B-pH proxy.

Sample	Species	Depth (m)	Seawater parameters					
			Temp (°C)	Salinity	pH_T	Alk (μmol/kg)	Ω_{arag} (calc*)	Source
Tasman Seamount								
Hill_B1	*D. dianthus*	1050	4.59	34.4	7.87	2315	1.02 ± 0.04	Seawater measured
Marmara Sea								
DD_MS	*D. dianthus*	932	14.50	38.8	7.77	2610	1.46 ± 0.02	Seawater measured
Chilean Fjord								
DD_7	*D. dianthus*	25–35	10.87	31.7	7.83	2136	1.19 ± 0.02	Seawater measured
Mediterranean Sea								
MedCor-25-D	*D. dianthus*	462–690	13.78	38.75	8.10	2613	2.88 ± 0.09	Seawater measured
MedCor-74-D	*D. dianthus*	824–850	13.96	38.77	8.05	2624	2.59 ± 0.07	Seawater measured
MedCor-41-CA	*C. smithii*	139	16.00	38.22	8.09	2564	3.09 ± 0.07	Seawater measured
MedCor-57-CA	*C. smithii*	89	16.76	37.76	8.09	2520	3.14 ± 0.14	Seawater measured
MedCor-59-CA	*C. smithii*	117	16.51	38.04	8.09	2564	3.09 ± 0.07	Seawater measured
MedCor-25-L	*L. pertusa*	462–690	13.78	38.75	8.10	2613	2.88 ± 0.09	Seawater measured
MedCor-74-L	*L. pertusa*	824–850	13.96	38.77	8.05	2624	2.59 ± 0.09	Seawater measured
MAL: Malta	*L. pertusa*	452–607	13.82	38.71	8.10	2613	2.88 ± 0.09	Seawater measured
GS: M70/1–752 (D111)	*L. pertusa*	674–710	13.55	38.64	8.08	2600	2.70 ± 0.09	GLODAP/CARINA
NE Atlantic Ocean								
SR: POS-228–216	*L. pertusa*	250–320	7.52	35.17	8.03	2305	1.72 ± 0.05	GLODAP/CARINA
DW: 13831 #1	*L. pertusa*	950	6.31	35.20	8.06	2323	1.82 ± 0.07	GLODAP/CARINA
GB: VH-97-351	*M. oculata*	775–880	10.90	35.87	7.99	2363	1.80 ± 0.03	GLODAP/CARINA
PM: POS-265-449	*L. pertusa*	729	9.60	35.48	7.98	2333	1.63 ± 0.16	GLODAP/CARINA
RB: POS-292-544-1	*L. pertusa*	835–858	7.92	35.23	8.00	2309	1.60 ± 0.08	GLODAP/CARINA
N Pacific Ocean:								
PV703_Cor_5	*Corallium* sp.	942	4.07	34.50	7.66	2370	1.03* ± 0.05	GLODAP
PV703_Enal_2	*E. rostrata*	1108	3.54	34.53	7.69	2387	0.67 ± 0.05	GLODAP
PV703_Enal_7	*E. rostrata*	534	5.74	34.19	7.64	2309	0.70 ± 0.02	GLODAP

Abbreviations of genus names: *C* = *Caryophyllia*, *D* = *Desmophyllum*, *E* = *Enallopsammia*, *L* = *Lophelia*, *M* = *Madrepora*.
* Indicates that Ω refers to calcite in *Corallium* sp.

On this basis the equation used to convert the $\delta^{11}B_{carb}$ isotopic composition measured in the coral carbonate skeleton to a pH value (Zeebe and Wolf-Gladow, 2001) of the calcifying fluid (pH_{cf}) is given by:

$$pH_{cf} = pK_B - \log\{[\delta^{11}B_{sw} - \delta^{11}B_{carb}]/\{[\alpha_{(B3-B4)}\delta^{11}B_{carb} - \delta^{11}B_{sw} + 1000(\alpha_{(B3-B4)} - 1)]\}\} \quad (4)$$

where $\delta^{11}B_{sw}$ and $\delta^{11}B_{carb}$ represent the $\delta^{11}B$ in seawater ($\delta^{11}B_{sw} = 39.61‰$) (Foster et al., 2010) and in carbonate respectively, and $\alpha_{(B3-B4)} = 1.0272$ (as discussed above). The dissociation constant of boric acid pK_B has a well-established value of 8.597 at 25 °C and a salinity of 35 (Dickson, 1990). For cold deep-water corals, temperature and pressure corrections are also applied (Zeebe and Wolf-Gladow, 2001; Rae et al., 2011) using coefficients from CO2SYS Matlab version 1.1 (Lewis and Wallace, 1998).

The assumption that only the borate ion is partitioned into the calcium carbonate skeleton of biogenic calcifiers has recently been questioned, based on significant quantities of boric acid species observed from nuclear magnetic resonance and electron-loss spectroscopy (Klochko et al., 2009; Rollion-Bard et al., 2011). These studies reported variable proportions (12–48%) of the trigonally co-ordinated $B(OH)_3$ in different skeletal components of the carbonate skeletons of corals. If significant proportions of the trigonally coordinated $B(OH)_3$ are directly incorporated during calcification, then the boron isotopic composition would shift to considerably higher values, more characteristic of the $B(OH)_3$ end-member composition. The boric species in the calcifying medium, with a normal range of seawater pH_T (e.g. 7.8–8.2), would have a $\delta^{11}B$ composition between ~43‰ and 47‰ if in equilibrium with seawater. Incorporation of variable quantities of $B(OH)_3$ at a particular pH would however result in vertical mixing arrays between $\delta^{11}B_{carb}$ and seawater pH, with borate being the low $\delta^{11}B$ end-member and the boric $B(OH)_3$ species being the high $\delta^{11}B$ end-member component. A model of $B(OH)_3$ incorporation into the coral skeleton (Fig. 3) shows the dependence on relative concentration (i.e. distribution coefficient), and that the $\delta^{11}B_{carb}$ composition (and total B concentration) would increase rapidly with decreasing pH as the proportion of $B(OH)_3$ increases. Thus, the addition of the boric species should produce a distinct, strongly curvilinear array in $\delta^{11}B_{carb}$ versus seawater pH plots, rather than the highly correlated approximately linear arrays observed herein and by Trotter et al. (2011). Furthermore, modelling (Fig. 3) indicates a K_d for boric substitution of <0.1, which is significantly less than that needed to account for the quantities

observed in the NMR studies (Klochko et al., 2009; Rollion-Bard et al., 2011).

The relationship between $\delta^{11}B_{carb}$ and seawater pH therefore provides a sensitive means for assessing the stoichiometric incorporation of $B(OH)_3$ relative to $B(OH)_4^-$. Alternatively, if additional $B(OH)_3$ was incorporated with $B(OH)_4^-$ (Eq. (3)), into the $CaCO_3$ skeleton, it may be that this occurs without further isotopic fractionation of boric relative to the borate species. A set of possible reactions has also been proposed by Klochko et al. (2009). The presence of the boric species may thus be inconsequential, as the boron isotope systematics appears to be controlled by the borate composition. In the following section we show that the $\delta^{11}B_{carb}$ compositions of the cold-water coral *D. dianthus* relative to seawater pH_T also forms a highly correlated array similar to that reported for tropical and sub-tropical corals (Trotter et al., 2011). We show that this pattern is consistent with isotope fractionation controlled by the borate species together with a highly systematic physiological process that regulates 'internal' (extracellular) pH of the calcifying fluid (pH_{cf}) during precipitation of the carbonate skeleton, rather than variable uptake of the $B(OH)_3$ species.

2.4. Boron isotope systematics of biological (internal) pH up-regulation

The calcification mechanisms illustrated schematically in Fig. 1 indicate that the $\delta^{11}B_{carb}$ compositions of aragonitic corals represent ambient seawater pH with the superimposed effects of biological pH up-regulation at the site of calcification. This is not unexpected as it is well known that corals internally up-regulate pH (Al-Horani et al., 2003; Marubini et al., 2008), although quantification of this process by *in situ* measurements are still limited (Ries, 2011; Venn et al., 2011). The $\delta^{11}B_{carb}$ composition of carbonate skeletons therefore provides quantitative constraints on the average pH_{cf} at the site of calcification during this biologically-mediated process. A linear relationship (Trotter et al., 2011) between the biologically controlled internal pH_{cf} and external seawater pH_T is shown schematically in Fig. 3 and defined by:

$$pH_{cf} = m(pH_T) + C_{sp} \quad (5)$$

where m is the gradient of the linear array and C_{sp} denotes the species dependent value of the intercept.

The biological up-regulation or differential pH (ΔpH) relative to ambient seawater at the site of calcification is expressed as:

$$\Delta pH = pH_{cf} - pH_T \quad (6)$$

and from Eqs. (5) and (6) this corresponds to the relationship:

$$\Delta pH = (m-1)pH_T + C_{sp} \quad (7)$$

Thus linear correlations between either pH_{cf} or ΔpH versus seawater pH_T is indicative of systematic pH up-regulation (Fig. 3b).

3. RESULTS

Boron isotope measurements ($\delta^{11}B_{carb}$) were determined for a suite of cold-water azooxanthellate corals from various ocean basins and collected over a large range of depths. They comprise the aragonite species, *C. smithii*, *D. dianthus*, *E. rostrata*, *L. pertusa*, and *M. oculata*, as well as the calcitic coral, *Corallium* sp. An important aspect of this study is that the $\delta^{11}B_{carb}$ data are complemented with well-constrained seawater pH_T measurements for *D. dianthus*, or reasonable quantitative estimates (with noted caveats) for the other corals, which are essential to define the systematics of biologically mediated pH regulation (Table 2).

The $\delta^{11}B_{carb}$ compositions plotted against seawater pH_T (Fig. 4) show that all aragonitic cold-water coral samples lie significantly above the $B(OH)_4^-$ speciation curve of Klochko et al. (2006). To better illustrate the range of biological controls, we plot these data (Fig. 5) using both the boron-derived pH_{cf} (Fig. 5a) and the ΔpH versus seawater pH_T (Fig. 5b) following Eqs. (5) and (7). Using the approach of Trotter et al. (2011) and the boron isotope systematics outlined above, a correlated linear relationship ($r^2 = 0.79$, $n = 6$) is found for *D. dianthus* where:

$$pH_{cf} = 0.29pH_T + 6.43 \quad (8)$$

or

$$\Delta pH_{Desmo} = 6.43 - 0.71pH_T \quad (r^2 = 0.79) \quad (9)$$

At the nominal value of seawater $pH_T = 8.0$, *D. dianthus* is thus offset by ~0.8 ΔpH units above ambient seawater (Fig. 5b). Their general consistency is also notable,

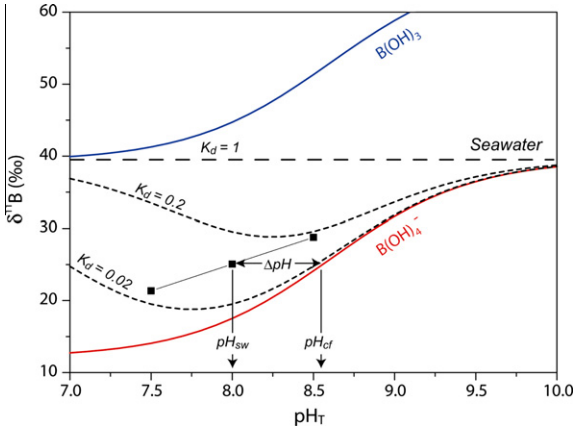

Fig. 3. Schematic diagram showing the relationship between $\delta^{11}B$ measured in corals (solid squares) and seawater pH_T. Biologically mediated internal pH_{cf} up-regulation at the site of calcification is characterised by pH_{cf} being greater than seawater pH, and follows a highly systematic approximately linear relationship of $pH_{cf} = m\,pH_{sw} + c$. Also shown is an alternative model for incorporation of both boric and borate species with a constant distribution coefficient (K_d) between the crystallizing medium and carbonate skeleton, which produces strongly curvilinear arrays (dashed lines) that is inconsistent with the observations (e.g. solid squares) of this study and by Trotter et al. (2011). Variable contributions of the boric component at a constant pH would be expected to produce vertical mixing arrays (Fig. 2b).

especially given their disparate and contrasting provenances from shallow-water fjords (Chile), a high salinity restricted ocean basin (Marmara Sea), their deep water habitats in the North Atlantic and Southern oceans that together encompass depths ranging from ~30 to ~1100 m, and that not all seawater samples were taken specifically at the coral site. The exception is the sample from the southern ocean that has a comparatively higher ΔpH_{cf}. The other species of aragonitic cold-water corals analysed typically have slightly higher ΔpH values (up to ~1), with *L. pertusa* also defining an approximately linear array but, due to the limited range of pH_T, is still poorly defined ($r^2 = 0.71$). Lying along the same trend but at a lower pH_T is the aragonitic *E. rostrata*, which is represented by two distinct morphotypes – a shallower robust form with thick branches (PV703_En-7) and deeper dwelling colony comprising delicate corallites (PV703_En-2) that could represent different species.

The ΔpH values calculated for these species using seawater values sourced from public databases (Table 1), as well as our estimates based on water column analyses, must however be taken with some caution as they may differ from ambient seawater pH at the actual coral site. For instance, an uncertainty in the pCO_2 in which the corals live of ±100 ppm would translate into an uncertainty of ±0.1 in seawater pH. Likewise, benthic boundary layer effects may also give rise to significant local variations in seawater pH. Another consideration is the effectiveness of the sub-sampling protocol for boron isotope analysis, as it can be difficult to avoid skeletal material from the centres of calcification in species comprising small corallites in particular. As shown by ion-probe analyses (Blamart et al., 2007), centres of calcification can have different $\delta^{11}B_{carb}$ values that could potentially confound the bulk sample boron isotope systematics. Further work is therefore required to better constrain the relationship between pH_{cf} versus seawater pH_T and Ω_{arag} (see discussion) for these and other species. This includes improved sampling protocols as well as accurate measurements of ambient seawater pH to help clarify the suitability of these species as potential archives of seawater pH. Where possible, comparative studies of boron derived and *in situ* (intra-polyp) pH_{cf} measurements of living and cultured corals will also be useful. Despite these issues, this suite of aragonitic cold-water coral species collectively show an overall trend of higher ΔpH values that is anti-correlated (Fig. 2b) with seawater pH_T, with systematics generally consistent with biologically controlled pH up-regulation.

Preliminary data for the calcitic cold-water coral *Corallium* sp. differ markedly from the boron isotope systematics of the aragonitic species *E. rostrata* collected from the same site. *Corallium* sp. has a much lower $\delta^{11}B_{carb}$ composition (~15.5 ± 0.2‰) as well as B concentration and, using a

Table 2
Boron isotope compositions of cold-water corals and seawater pH_T measurements. Isotope measurements were normalised to SRM951 and are expressed as delta values ($\delta^{11}B$), and external precision is 0.31‰ based on our in-house coral *Porites* standard (NEP). Typical errors for ΔpH are 0.02 units or better with pH_{cf} and ΔpH having errors of <0.01 unit (see text).

Sample	Species	$\delta^{11}B_{carb}$ (‰)	2sem	pH_{cf} (internal)	pH_T (seawater)	ΔpH
Tasman Seamount						
Hill_B1	*Desmophyllum dianthus*	26.14	0.08	8.83	7.87	0.96
Marmara Sea						
DD_MS (subs 1)	*Desmophyllum dianthus*	25.68	0.07	8.66	7.77	0.89
DD_MS (subs 2)	*Desmophyllum dianthus*	25.87	0.03	8.67	7.77	0.90
Chilean Fjord						
DD_7	*Desmophyllum dianthus*	24.50	0.06	8.71	7.83	0.88
Mediterranean Sea						
MedCor-25-D	*Desmophyllum dianthus*	27.36	0.05	8.79	8.10	0.69
MedCor-74-D	*Desmophyllum dianthus*	26.80	0.03	8.74	8.05	0.69
MedCor-41-CA	*Caryophyllia smithii*	27.90	0.05	8.82	8.09	0.73
MedCor-57-CA	*Caryophyllia smithii*	27.43	0.03	8.79	8.09	0.70
MedCor-59-CA	*Caryophyllia smithii*	28.69	0.08	8.87	8.09	0.78
MedCor-25-L	*Lophelia pertusa*	27.42	0.02	8.80	8.10	0.70
MedCor-74-L	*Lophelia pertusa*	28.68	0.03	8.86	8.05	0.81
MAL: Malta	*Lophelia pertusa*	28.14	0.03	8.84	8.10	0.74
GS: M70/1-752 (D 111)	*Lophelia pertusa*	27.49	0.04	8.80	8.08	0.72
NE Atlantic Ocean						
SR: POS-228-216	*Lophelia pertusa*	26.62	0.05	8.86	8.03	0.83
DW: 13831 #1	*Lophelia pertusa*	27.12	0.03	8.87	8.06	0.81
GB: VH-97-351	*Madrepora oculata*	27.86	0.08	8.86	7.99	0.87
PM: POS-265-449	*Lophelia pertusa*	26.79	0.08	8.82	7.98	0.84
RB: POS-292-544-1	*Lophelia pertusa*	28.35	0.04	8.93	8.00	0.93
N Pacific Ocean						
PV703_Cor_5	*Corallium* sp.	15.47	0.21	7.97	7.66	0.31
PV703_Enal_2	*Enallopsammia rostrata*	24.99	0.06	8.76	7.69	1.07
PV703_Enal_7	*Enallopsammia rostrata*	23.22	0.05	8.66	7.64	1.02

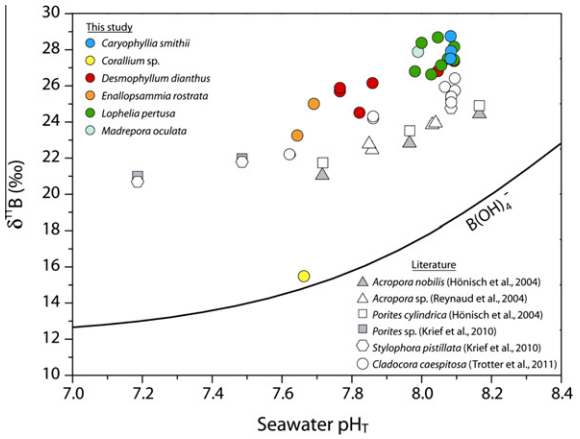

Fig. 4. Measured boron isotopic compositions ($\delta^{11}B_{carb}$) of cold-water corals (coloured symbols) plotted against seawater pH_T. Measurements of tropical corals from the literature (see legend) are represented by grey or open symbols. The black curve represents the $\delta^{11}B$ composition of the borate species $[B(OH)_4^-]$ as a function of seawater pH, assuming the boric/borate isotopic fractionation factor of 1.0272 (Klochko et al., 2006); $T = 25$ °C, $S = 35$, depth = 5 m. Aragonitic cold-water corals have significantly higher $\delta^{11}B_{carb}$ compositions than their tropical sub-tropical counterparts (grey symbols), indicative of greater extracellular pH up-regulation. The calcitic cold-water coral *Corallium* sp. lies near the borate curve suggesting that pH up-regulation is minimal or absent. Errors are within symbol size.

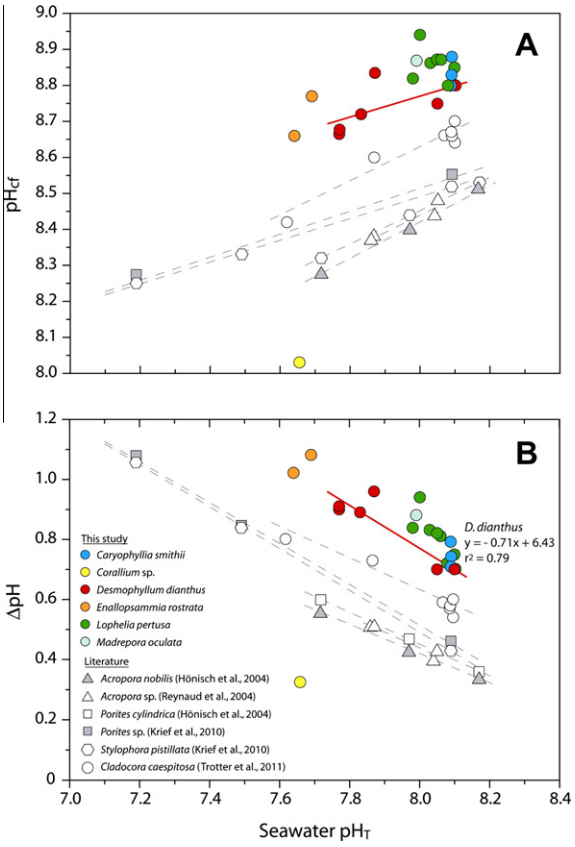

Fig. 5. (A) Internal pH_{cf} relative to ambient seawater pH_T for cold-water aragonitic corals and the calcitic *Corallium* sp. The excellent sub-parallel linear arrays for *Cladocora caespitosa* and tropical species *Porites*, *Acropora*, and *Stylophora* (Trotter et al., 2011) indicates that aragonitic corals have highly systematic physiological controls on their internal pH at the site calcification. (B) Seawater pH_T versus ΔpH of cold-water corals, where $\Delta pH = pH_{cf} - pH_{sw}$. At the same seawater pH, cold-water corals have ΔpH values up to ~0.5 pH unit higher than tropical corals. The cold-water corals *Desmophyllum dianthus* ($r^2 = 0.79$) and *Lophelia pertusa* ($r^2 = 0.71$) show approximate linear correlations of ΔpH with seawater pH_T, indicative of a systematic process of extracellular pH up-regulation. The less coherent data for some of the other species may be due to non-representative seawater pH estimates especially those from public databases, species effects, and/or the presence of more complex physiological processes.

seawater pH_T value sourced from the GLODAP database, has a significantly lower ΔpH value (~0.3) that approximates zero when extrapolated to a seawater pH_T of 8 and assuming a slope of ~1/2 as observed in aragonitic corals. Interestingly, this is within the ΔpH versus seawater pH_T arrays for calcitic foraminifera but at a much lower seawater pH_T. Taken at face value, this suggests that calcitic cold-water corals, like some species of calcitic foraminifera, may have a much reduced ability to up-regulate their internal pH.

4. DISCUSSION

The ΔpH relative to seawater pH_T relationships of different aragonitic coral groups (Fig. 5b) shows that azooxanthellate cold-water corals have the highest ΔpH values of ~0.8 to 1.0 measured thusfar at a reference seawater pH_T value of 8.0, whereas tropical shallow-water species approximate 0.4–0.5 (Fig. 5). The markedly higher ΔpH values of cold-water aragonitic corals have important implications for their resilience to environmental change driven by the combined effects of ocean acidification and global warming, which we examine below.

4.1. Up-regulation of internal pH_{cf} and aragonite saturation state (Ω_{cf}) of corals

Our new results for cold-water corals, together with recently published work (Trotter et al., 2011), provide new insights into pH up-regulation by corals. As shown in Eq. (9), *D. dianthus* maintains an approximately constant gradient between changes in seawater pH_T and its extracellular pH_{cf} at the site of calcification, as previously shown for temperate and tropical coral species (Trotter et al., 2011). This implies that pH regulation is driven by physiological processes similar to those that occur in the warm water hyper-calcifying zooxanthellate corals.

The ability of corals to up-regulate pH_{cf} at the site of calcification is important as calcification is ultimately controlled by the reaction $Ca^{2+} + CO_3^{2-} \rightarrow CaCO_3$, and in seawater CO_3^{2-} is the limiting ion concentration where CO_3^{2-} ~200 to 250 μmol kg^{-1} compared to Ca^{2+} ~10,000 μmol kg^{-1}. At the normal range of seawater pH, DIC is predominantly HCO_3^- (seawater HCO_3^- ~1800 μmol kg^{-1}), so increasing pH greatly enhances CO_3^{2-} concentrations by favouring the forward reaction of $HCO_3^- \rightarrow CO_3^{2-} + H^+$.

Similarly, within the biologically mediated calcifying medium, the major control on calcification is the internal saturation state (Ω_{cf}):

$$\Omega_{cf} = [Ca^{2+}]_{cf}[CO_3^{2-}]_{cf}/K_{spx} \quad (10)$$

where $[Ca^{2+}]_{cf}$ and $[CO_3^{2-}]_{cf}$ are the concentrations of dissolved calcium and carbonate ion at the site of calcification and K_{spx} is the solubility constant for either aragonite or calcite.

Following the standard reactions of the carbonate system in seawater, the relationship between the internal biologically mediated saturation state (Ω_{cf}) and internal pH_{cf} is given by:

$$\Omega_{cf} = [DIC]_{cf}[Ca^{2+}]_{cf} \Big/ K_{spx} \left\{ 1 + [H^+]_{cf} \Big/ K_2^* + [H^+]^2 \Big/ K_1^* K_2^* \right\} \quad (11)$$

where $pH_{cf} = -\log[H^+]_{cf}$, K_1^* and K_2^* are the stoichiometric equilibrium constants of the seawater carbonate system given by $K_1^* = [HCO_3^-][H^+]/[CO_2]$ and $K_2^* = [CO_3^{2-}][H^+]/[HCO_3^-]$, with the total concentration of dissolved inorganic carbon $[DIC]_{cf} = [CO_2]_{cf} + [HCO_3^-]_{cf} + [CO_3^{2-}]_{cf}$.

From the above equation, Ω_{cf} is thus strongly dependent on both pH_{cf} as well as the overall magnitude of the internal DIC enrichment relative to seawater. Currently, there are no direct measurements of internal $[DIC]_{cf}$ in corals, with the major enrichment mechanism being via diffusion-limited enrichment of CO_2 into the sub-calicoblastic space (Fig. 1), which at elevated pH may be insignificant especially for azooxanthellate (i.e. non-photosynthetic) cold-water corals.

The process of up-regulation of extracellular pH_{cf}, hence Ω_{cf}, as a function of seawater pH_T is calculated using Eq. (11) for *D. dianthus*, based on its pH_{cf} versus seawater pH_T calibration (Eq. (8)). This is shown in Fig. 6 where we assume $[DIC]_{cf} \sim [DIC]_{seawater}$, which implies replenishment of the internal DIC pool via repeated exchange with seawater. Alternate models are possible, such as constant $[DIC]_{cf}$, but these result in only subtle differences at the projected range of seawater pH. Thus within the typical environmental conditions for cold-water corals where seawater pH_T ranges from ~7.5 to 8.2, pH_{cf} up-regulation of up to 1 pH unit results in an associated increase in Ω_{cf} by a factor of 5- to 10-fold relative to ambient seawater. This is consistent with recent studies (Cohen et al., 2009; Holcomb et al., 2009) which also indicate high Ω_{cf} values. Importantly, the internal (extracellular) saturation state of cold-water corals is significantly greater than that for either inorganic aragonite or calcite, thereby greatly enhancing the potential rate of biomineralisation of their carbonate skeleton, as well as facilitating skeletal growth below the aragonite saturation horizon.

An alternative approach is to consider the observed relationships between pH_{cf} and seawater Ω_{arag} rather than the closely related parameter of seawater pH_T (Eq. (11)). This may provide an additional constraint on Ω_{cf} as samples have been obtained over a range of seawater DIC, the latter being largely independent of pH_T. This is shown in Fig. 7 where there is a good linear correlation between ΔpH and seawater Ω_{arag}, and is especially evident for *D. dianthus*

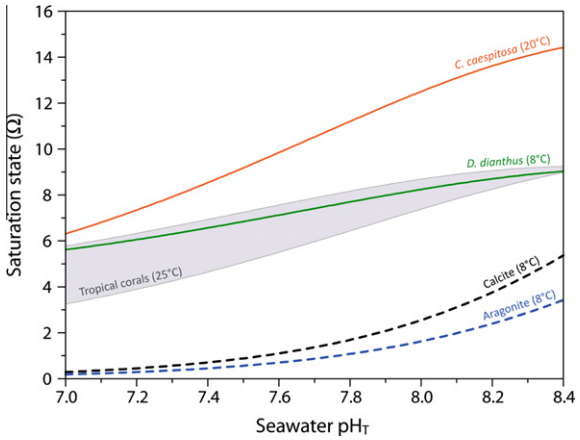

Fig. 6. Saturation states of coral calcifying fluid (Ω_{cf}) compared to inorganic saturation states for aragonite and calcite ($\Omega_{arag/calcite}$) over a range of seawater pH_T. Saturation states of the calcifying fluids (Ω_{cf}) are derived from boron isotopic systematics (Fig. 5) and shown for cold-water (*D. dianthus*, 8 °C), temperate (*C. caespitosa*, 20 °C) and tropical (25 °C) corals. As a consequence of biologically mediated pH up-regulation, Ω_{cf} values are all significantly greater than those for inorganic aragonite and calcite in ambient seawater. In contrast the calcitic species *Corallium* sp. has much lower Ω_{cf} overlapping with the inorganic calcite trajectory and hence lower rates of calcification (Fig. 8) Calculations of the calcifying fluid Ω_{cf} assume $[DIC]_{cf} \sim [DIC]_{seawater}$ with salinities of 35 for cold-water and tropical corals and 38 for temperate corals. Calculations are for cold-water corals at a depth of 500 m and for tropical and temperate corals at a depth of 5 m.

where $\Delta pH = 1.09 - 0.14\Omega_{arag}$ ($r^2 = 0.95$). This excellent linear correlation appears to be distinct from the curvilinear array or arrays (depending on DIC) that are expected for ΔpH versus seawater pH_T for the *D. dianthus* calibration (Eqs. (9) and (11)). This improved correlation of ΔpH with seawater Ω_{arag} indicates that the process of pH_{cf} up-regulation is more closely related to Ω_{cf}, the parameter that ultimately determines calcification rates (see following). Thus, the good correlation between pH_{cf} and seawater Ω_{arag} suggests that cold-water corals cannot manipulate pH_{cf} independent of Ω_{cf}, by for example increasing internal DIC. Importantly however, if we assume that $[DIC]_{cf}$ is relatively constant as outlined above, then this implies that via adjustments to pH_{cf}, Ω_{cf} is regulated to a relatively narrow range from ~8.5 to 12.5; this is interpreted as the Ω_{cf} threshold for calcification by azooxanthellae corals.

The good correlation between ΔpH and seawater Ω_{arag} and to a lesser extent with pH_T for *D. dianthus* and *L. pertusa* is also strong supporting evidence that their skeletal B isotopic signature is controlled by the borate species. This is because the boric acid species has highly enriched $\delta^{11}B$ values (Fig. 3) at ambient seawater pH_T values (~7.6 to 8.2), so plots of ΔpH against seawater Ω_{arag} or pH_T would define near vertical mixing arrays if boric acid was present in any significant quantity. For the *D. dianthus* and *L. pertusa* arrays, the range in $\delta^{11}B$ at the same seawater pH_T limits incorporation of $B(OH)_3$ to <5%, much less than that inferred by Rollion-Bard et al. (2011) where 18–48% was identified in the fibres and calcification centres respectively.

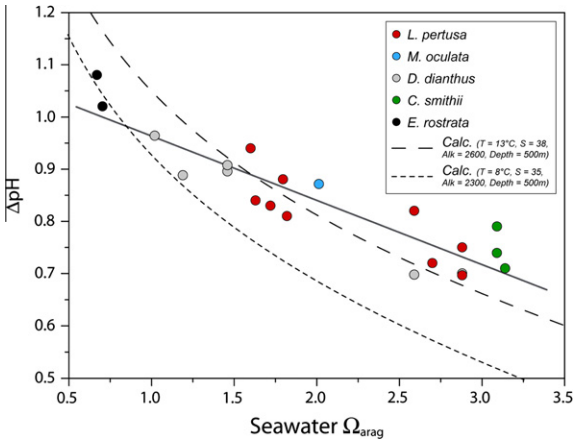

Fig. 7. Plot of ΔpH versus the seawater aragonite saturation state Ω_{arag}. The curved dashed lines show the expected relationship for Alk = 2300 μmol kg^{-1} (small dash) and 2600 μmol kg^{-1} (large dash) calculated for *D. dianthus* (Eq. (9)). There is a good correlation ($r^2 = 0.95$) between ΔpH and seawater Ω_{arag} for the cold-water coral species *D. dianthus* consistent with $[DIC]_{cf}$ of the calcifying fluid being similar to seawater DIC, with the observed ΔpH range defining the limits of internal Ω_{cf} from ~8 to 13 within the calcifying fluid (see Fig. 6).

Furthermore, the high proportions of $B(OH)_3$ in the calcification centres had lower rather than higher $\delta^{11}B$ compositions (Rollion-Bard et al., 2011), contrary to the systematics described in Fig. 2. We therefore conclude that the inherently consistent $\delta^{11}B$ systematics of deep-sea corals is primarily controlled by the pH-dependent incorporation of borate ions that have a pH-dependent isotopic composition.

4.2. Calcification rates of cold-water corals

To quantify how biological pH up-regulation effects calcification rates we use the empirical exponential rate dependence law for abiotic carbonate precipitation (Burton and Walter, 1987), but applied to the biologically mediated internal saturation state Ω_{cf} such that:

$$R_{calcif} = k(\Omega_{cf} - 1)^n \quad (12)$$

where R_{calcif} is the rate of calcification, k is the rate law constant, and n is the order of the reaction with the following temperature-dependence for aragonite (Burton and Walter, 1987):

$$k_{arag} = -0.0177T^2 + 1.47T + 14.9$$

$$n_{arag} = 0.0628T + 0.0985$$

and for calcite precipitation:

$$k_{calcite} = 0.0153T^2 - 0.968T + 18.4 \quad \text{for } T < 25°C$$

$$k_{calcite} = -0.0167T + 4.32 \quad \text{for } T \geq 25°C$$

This approach, based on the concept of 'biologically induced' calcification (Lowenstam and Weiner, 1989), combines **I**nternal **pH** **R**egulation with **A**biotic **C**alcification, which we term IpHRAC. Our model thus provides a quantitative means to determine relative changes in calcification rates as a function of both ambient seawater pH_T and temperature. In this model we have set two representative temperatures for *D. dianthus* at 4 and 12 °C, and a salinity of 35. Absolute calcification rates can also be calculated using these parameters, with Ω_{cf} modelled either as a function of seawater aragonite saturation state or seawater pH_T (Fig. 8).

Using our IpHRAC model, the calcification rate (R_{calcif}) for *D. dianthus* shows a strong sensitivity to temperature, with rates of ~0.2 mmol $CaCO_3$ m^{-2} h^{-1} at 12 °C, compared to ~0.03 mmol $CaCO_3$ m^{-2} h^{-1} at 4 °C, this being due to the strong temperature dependence of the rate constant (k) and reaction order (n) for aragonite precipitation. This is broadly consistent with results based on direct measurements of R_{calcif} for *D. dianthus* using U-series dating of extension rates (Cheng et al., 2000; Adkins et al., 2004; Montagna et al., 2006). These show that corals living in higher temperature environments, such as the Mediterranean (~14 °C), have up to one order of magnitude faster extension rates (~1 mm/yr) compared to those in the colder (~4 °C) deep-waters of the Pacific Ocean (<0.2 mm/yr). For instance, given an average pH_T of 8.08 (Table 2) and a Total Alkalinity (TA) of ~2600 μmol kg^{-1} for the Mediterranean, and a pH_T of 7.9 and TA of ~2200 μmol kg^{-1} for the cold-water coral studied by Adkins et al. (2004) and Cheng et al. (2000), the IpHRAC model would predict that growth rates in the Mediterranean would be 2- to 4-fold higher than in the deep Pacific Ocean; these differences are broadly consistent with observed rates (Cheng et al., 2000; Adkins et al., 2004; Montagna et al., 2006). To first order, it is therefore the relatively high internal saturation state combined with the strong temperature control on the kinetics of aragonite precipitation that control the inorganic calcification rates in *D. dianthus* and cold-water corals generally.

Nevertheless, it is also apparent that other factors, such as food supply, play a crucial role in the calcification process of cold-water corals. This is exemplified by the relatively rapid growth of cold-water corals in fjords, such as Chile at ~11 °C (Försterra et al., 2005), where higher particle supply, hence nutrient levels, from melt-water streams combined with micro-endolithic phototrophic organisms (Försterra and Häussermann, 2008) result in markedly faster growth rates (3–4 mm/yr) compared to the mostly oligotrophic but similar temperature waters (12–14 °C) of the Mediterranean deep waters. It is therefore clear that the over-riding control on calcification rates is ultimately the physiological limitations of azooxanthellate cold-water corals, in particular their limited ability to harness the energy essential for enzyme driven ion transporters and effective operation of the Ca^{2+}-ATPase for pH up-regulation.

The importance of energy limitations on the physiological control of internal pH_{cf} can be estimated from relative energy requirements needed to maintain the extracellular pH gradient between seawater and the calcification site. This can be readily quantified since the free energy needed to maintain the ΔpH gradient is given by:

$$\Delta G_{H+} = 2.3\, RT\Delta pH \quad (13)$$

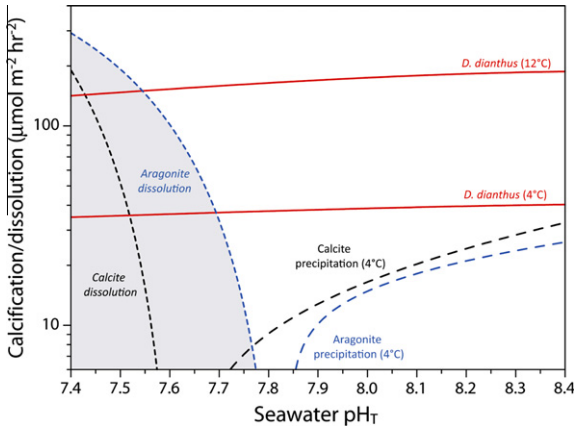

Fig. 8. Calcification and dissolution rates of calcite and aragonite (shaded zone is aragonite under-saturation) plotted as a function of seawater pH_T. Internal pH_{cf} up-regulation of the calcifying fluid by *Desmophyllum dianthus* (red lines) results in significantly faster rates of calcification compared to inorganic aragonite (blue dashed line) at the same temperature. Strong controls on both extracellular pH_{cf} and hence Ω_{cf} in cold-water corals indicate that the effects of ocean acidification may largely be countered by enhanced rates of calcification due to warming of the deep oceans. The viability of deep-sea corals in the context of ongoing ocean acidification is thus mainly determined by the sensitivity of skeletal dissolution rates to decreasing seawater pH, which occurs below the saturation horizon, combined with the additional energetic cost to maintain increasing pH gradients. (For interpretation of the references to colour in this figure legend, the reader is referred to the web version of this article)

where R is the gas constant (8.314 J K^{-1} mol^{-1}) and T is the temperature in Kelvin.

Thus for a typical value of ΔpH ~0.8 (Fig. 5b), the free energy change needed to maintain the pH gradient between the extracellular site of calcification (pH_{cf}) and seawater (pH_T) is ΔG_{H+} ~5 kJ mol^{-1} H^+ transported. For metabolic carbon provided in the form of bicarbonate, the coral would need to pump only 1 H^+ mol^{-1} of $CaCO_3$ precipitated. With pH up-regulation, a major decrease in seawater pH_T of 0.1 unit would increase ΔpH by only ~0.07 units (i.e. to ΔpH of ~0.87; Fig. 5b), requiring only ~10% more energy equivalent to ~0.5 kJ mol^{-1} of H^+ pumped. Whilst not a major increase, due to an absence of zooxanthellae and hence generally more restricted energy resources, this may be a significant physiological limitation of azooxanthellae corals, leading to slower growth rates. So although cold-water corals calcify at a similar internal saturation states compared to tropical corals, it is the lack of zooxanthellae that imposes energy limitations thus indirectly controlling calcification rate. It is therefore likely that azooxanthellate corals are generally restricted to dark and cold-water habitats (<14 °C) because they cannot compete effectively with the symbiont-bearing hyper-calcifying tropical corals of shallow-water photic environments.

Our findings that cold-water corals are characterised by high ΔpH values indicates that the energetics of elevating internal pH via Ca^{2+}-ATPase may be the singular rate-limiting step of azooxanthellate coral calcification. This is in contrast to hyper-calcifying tropical corals that appear to operate with significantly lower ΔpH values (Trotter et al., 2011). This suggests that there is a trade-off in energy utilisation between internal pH up-regulation and processes such as ion transport and the building of organic templates. We speculate that organic matrices or templates secreted by the coral during calcification (Cuif and Dauphin, 2005; Tambutté et al., 2007) are also important in controlling the species-dependent offset of ΔpH observed in the different scleractinian coral groups. These species-specific organic templates as well as other mechanisms (Meibom et al., 2007) may, for example, serve to suppress calcification until a minimum site-specific threshold of Ω_{cf} is reached. As a consequence, crystal lattice-scale variations in saturation state and hence pH_{cf} may be expected to occur between the centres of calcification and fibrous aragonite, as inferred by $\delta^{11}B_{carb}$ measured at high spatial resolution by ion micro-probe (Blamart et al., 2007), as well as small-scale correlated co-variations in $\delta^{18}O$ and $\delta^{13}C$ (Adkins et al., 2003).

4.3. Dissolution rates of cold-water corals

The ability of cold-water corals to elevate their saturation state Ω_{cf} at the site of calcification and thus calcify at, or in some cases below, the aragonite saturation horizon raises the importance of how the dissolution of coral exoskeletons are effected by seawater pH, and thus the potentially more corrosive environment due to declining seawater pH. Analogous to abiotic calcification, the empirical rate law for carbonate dissolution (Walter and Morse, 1985) is given by:

$$R_{dis} = k(1 - \Omega_{sw})^n \quad (14)$$

where Ω_{sw} is the seawater saturation state for either calcite or aragonite, log $k_{arag} = 2.99$ (μmol m^{-2} h^{-1}) and $n_{arag} = 2.50$ at 25 °C (for aragonite) and 1 atm total pressure, based on data for *Acropora*. For calcite we use log $k_{calcite} = 3.38$ (μmol m^{-2} h^{-1}) and $n_{calcite} = 2.74$ at 25 °C at 1 atm total pressure, based on normalisation to specific area for the calcite barnacle shell of *Balanus* (Walter and Morse, 1985). Using these parameters and $\Omega_{sw} < 1$, dissolution rates increase exponentially with decreasing seawater pH (Fig. 8). Although still semi-quantitative, given that empirical results are only available at 25 °C, with dissolution rates being slower at lower temperatures, they nevertheless provide a lower limit for seawater pH and hence an effective depth range of cold-water corals.

For many species, as exemplified by *D. dianthus*, the dissolution (and bio-erosion) rate of the skeletal 'hold-fast' is likely to be critical as it enables the coral to maintain their up-right habit or, in the case of the Chilean corals, a vertically hanging position for optimal feeding (Försterra et al., 2005). Accordingly, the dissolution rates of this exposed and crucial component of cold-water coral skeletons may be an important control on their longevity. As shown in Fig. 8, dissolution rates increase dramatically for seawater $pH_T < 7.8$, a consequence of seawater $\Omega < 1$. Thus small changes in seawater pH of ~0.1 pH units from 'acidification' of the deep oceans will greatly enhance dissolution rates of cold-water corals living near or below the aragonite saturation horizon. An important caveat is, however, that

this process is highly dependent on the relative surface area of exposed skeleton, the still poorly understood effects of surface coatings (e.g. the role of tissue, mucus and Mn coatings), as well as the largely unknown rates of bio-erosion at these particular depths and low temperatures.

5. CONCLUSIONS

Boron isotope systematics of aragonitic azooxanthellate cold-water corals indicates that, like symbiont-bearing tropical corals (Trotter et al., 2011), they have the ability to ameliorate or buffer external changes in seawater pH by up-regulating their pH_{cf} at the site of calcification. Importantly, we also show that the process of pH up-regulation in the cold-water coral *D. dianthus* correlates with variations in ambient seawater Ω_{arag} ($r^2 = 0.95$) and to a lesser extent with pH_T ($r^2 = 0.79$). Our finding that aragonitic cold-water corals have significantly higher ΔpH values than both tropical and temperate aragonitic species indicates that pH up-regulation is an important physiological process controlling calcification, by increasing the Ω_{cf} at the site of calcification. For cold-water corals, the extent of pH_{cf} up-regulation is also closely related to the seawater saturation state Ω_{arag}, and hence to Ω_{cf}, which ultimately controls calcification. This is a highly effective adaptive strategy to overcome the severe environmental limitations of the deep ocean, in particular the low seawater Ω_{arag}. This finding cogently explains how cold-water corals calcify at, or in some cases below, the aragonite saturation horizon, albeit with very slow annual growth rates at the micron to millimetre scale. The slower growth rates is attributed to the additional energy cost (~10% per −0.1 pH_T) needed to maintain a higher pH gradient (ΔpH) between seawater and the site of calcification, as well as the lower temperatures at greater depths.

Our IpHRAC (Internal pH Regulation Abiotic Calcification) model indicates that cold-water corals are likely to be much more resilient to decreasing seawater pH from ocean acidification than previously realised. Decreasing seawater pH alone will only marginally affect calcification rates since this process would be largely countered by pH_{cf} up-regulation in cold-water corals, together with enhanced calcification rates from warming of the deep oceans (Fig. 8). Other more difficult to quantify effects from ocean acidification, such as increased dissolution of tissue-free portions of the coral skeleton and the 'hold-fast' in particular, may have a more significant effect on the longer-term viability of cold-water corals, especially those growing near the saturation horizon.

Additional considerations include large-scale effects of climate change, such as a breakdown in the ocean's 'biological pump' (Feely et al., 2004; Orr et al., 2005) and consequent decrease in the supply of organic particles supporting present levels of heterotrophic metabolism. Furthermore, as deep ocean ventilation is inhibited by rapid global warming, there is likely to be decreased levels of dissolved oxygen that will have undesirable consequences for cold-water coral ecosystems. Such changes may have occurred at the end of the Younger Dryas period, which saw the rapid demise of deep-sea corals during warming of the Mediterranean, together with decreased deep-water circulation and changes to the supply of organic particles (McCulloch et al., 2010). These broader and more difficult to predict impacts of climate change may therefore play a critical role in the survival of cold-water corals.

ACKNOWLEDGMENTS

We thank Masters, Crew, Shipboard and Science Staff onboard RRVV *Urania* and *Meteor* during coral cruises in the Mediterranean Sea and the Atlantic Ocean. We gratefully appreciate the efforts of Ron Thresher (CSIRO) and Jess Adkins (Caltech) for helpful discussions and organising the ROV Jason expedition into the Southern Oceans and shipboard crew of the RV Thompson and Southern Surveyor. We thank the Hawai'i Underwater Research Laboratory (HURL) for access to the deep-diving submersibles, Pisces IV & V. Thanks are due to Jean-Claude Caprais, Bronte Tilbrook, and Rodrigo Torres for providing pH measurements from the Marmara Sea, Southern Ocean, and Comau Fjord, respectively; as well as Agostina Vertino for identifying the Mediterranean coral species. We thank Graham Mortimer for his invaluable assistance with the boron isotope analyses conducted at ANU. Partial funding was provided from the European Community's Seventh Framework Programme (FP7/2007-2013) under the HERMIONE project, Grant agreement n° 226354 and COCONET (Grant agreement 287844) projects. P. Montagna is grateful for financial support from the Marie Curie International Outgoing Fellowship (MEDAT-ARCHIVES). This work has been supported by Australian Research Council (ARC) Grant DP0986505 awarded to M. McCulloch and J. Trotter and essential support provided to M. McCulloch by the ARC Centre of Excellence in Coral Reef Studies and the award of a Western Australian Premiers Fellowship.

APPENDIX A. SUPPLEMENTARY DATA

Supplementary data associated with this article can be found, in the online version, at http://dx.doi.org/10.1016/j.gca.2012.03.027.

REFERENCES

Adkins J. F., Boyle E. A., Curry W. B. and Lutringer A. (2003) Stable isotopes in deep-sea corals and a new mechanism for "vital effects". *Geochim. Cosmochim. Acta* **67**(6), 1129–1143.

Adkins J. F., Henderson G. M., Wang S.-L., O'Shea S. and Mokadem F. (2004) Growth rates of the deep-sea scleractinian *Desmophyllum cristagalli* and *Enallopsammia rostrata*. *Earth Planet. Sci. Lett.* **227**(3), 481–490.

Al-Horani F. A., Al-Moghrabi S. M. and de Beer D. (2003) Microsensor study of photosynthesis and calcification in the scleractinian coral *Galaxea fascicularis*: active internal carbon cycle. *J. Exp. Mar. Biol. Ecol.* **288**(1), 1–15.

Allemand D., Ferrier-Pagès C., Furla P., Houlbrèque F., Puverel S., Reynaud S., Tambutté E., Tambutté S. and Zoccola D. (2004) Biomineralisation in reef-building corals: from molecular mechanisms to environmental control. *C.R. Palevol* **3**(6/7), 453–467.

Blamart D., Rollion-Bard C., Meibom A., Cuif J.-P., Juillet-Leclerc A. and Dauphin Y. (2007) Correlation of boron isotopic composition with ultrastructure in the deep-sea coral *Lophelia pertusa*: implications for biomineralization and paleo-pH. *Geochem. Geophys. Geosyst.* **8**(Q12001), 11.

Burton E. A. and Walter L. M. (1987) Relative precipitation rates of aragonite and Mg calcite from seawater: temperature or carbonate ion control? *Geology* **15**(2), 111–114.

Caldeira K. and Wickett M. E. (2003) Oceanography: anthropogenic carbon and ocean pH. *Nature* **425**(6956), 365.

Cheng H., Adkins J., Edwards R. L. and Boyle E. A. (2000) U–Th dating of deep-sea corals. *Geochim. Cosmochim. Acta* **64**(14), 2401–2416.

Cohen A. L. and Holcomb M. (2009) Why corals care about ocean acidification: uncovering the mechanism. *Oceanography* **22**(4), 118–127.

Cohen A. L. and McConnaughey T. (2003) Geochemical perspectives on coral mineralization. In *Biomineralization* (eds. P. Dove, S. Weiner and J. Yoreo). Rev. Mineral. Geochem. 54, 151–187.

Cohen A. L., McCorkle D. C., De Putron S., Gaetani G. A. and Rose K. A. (2009) Morphological and compositional changes in skeletons of new coral recruits reared in acidified seawater: insights into the biomineralization response to ocean acidification. *Geochem. Geophys. Geosyst.* **10**(7), 1–12.

Cuif J. P. and Dauphin Y. (2005) The environment recording unit in corals skeletons – a synthesis of structural and chemical evidence for a biochemically driven stepping-growth process in fibres. *Biogeosciences* **2**, 61–73.

Dickson A. G. (1990) Standard potential of the reaction: AgCl(s) + $1/2H_2(g) = Ag(s) + HCl(aq)$ and the standard acidity constant of the ion HSO_4^- in synthetic seawater from 273/15 to 318.15K. *J. Chem. Thermodyn.* **22**, 113–127.

Dickson A. G., Sabine C. L. and Christina J. R. (2007). Guide to best practices for ocean CO_2 measurements: PICES Special Publication 3, pp. 191.

Erez J. (2003) The source of ions for biomineralization in foraminifera and their implications for paleoceanographic proxies. In (eds. P. M. Dove, J. J. D. Yoreao and S. Weiner). Rev. Mineral. Geochem. 54, 115–149.

Fautin D. G., Guinotte J. M. and Orr J. C. (2009) Comparative depth distribution of corallimorpharians and scleractinians (Cnidaria: Anthozoa). *Mar. Ecol. Prog. Ser.* **397**, 63–70.

Feely R. A., Sabine C. L., Lee K., Berelson W., Kleypas J., Fabry V. J. and Millero F. J. (2004) Impact of anthropogenic CO_2 on the $CaCO_3$ system in the oceans. *Science* **305**(5682), 362–366.

Form A. U. and Riebesell U. (2012) Acclimation to ocean acidification during long-term CO2 exposure in the cold-water coral *Lophelia pertusa*. *Global Change Biol.* **18**, 843–853.

Försterra G. and Häussermann V. (2008) Unusual symbiotic relationships between microendolithic phototrophic organisms and azooxanthellate cold-water corals from Chilean fjords. *Mar. Ecol. Prog. Ser.* **370**, 121–125.

Försterra G., Beuck L., Häussermann V. and Freiwald A. (2005) Shallow-water *Desmophyllum dianthus* (Scleractinia) from Chile: characteristics of the biocoenoses, the bioeroding community, heterotrophic interactions and (paleo)-bathymetric implications, In *Cold-water Corals and Ecosystems* (eds. A. Freiwald and J. M. Roberts). Springer-Verlag, Berlin Heidelberg. pp. 937–977.

Foster G. L. (2008) Seawater pH, pCO_2 and $[CO_3^{2-}]$ variations in the Caribbean Sea over the last 130 kyr: a boron isotope and B/Ca study of planktonic forminifera. *Earth Planet. Sci. Lett.* **271**, 254–266.

Foster G. L., Pogge von Strandmann P. A. E. and Rae J. W. B. (2010) Boron and magnesium isotopic composition of seawater. *Geochem. Geophys. Geosyst.* **11**(8), Q08015.

Gattuso J.-P., Allemand D. and Frankignoulle M. (1999) Photosynthesis and calcification at cellular, organismal and community levels in coral reefs: a review on interactions and control by carbonate chemistry. *Am. Zool.* **39**, 160–183.

Guinotte J. M., Orr J. C., Cairns S., Freiwald A., Morgan L. and George R. (2006) Will human-induced changes in seawater chemistry alter the distribution of deep-sea scleractinian corals? *Front. Ecol. Environ.* **4**(3), 141–146.

Hemming N. G. and Hanson G. N. (1992) Boron isotopic composition and concentration in modern marine carbonates. *Geochim. Cosmochim. Acta* **56**, 537–543.

Holcomb M., Cohen A. L., Gabitov R. I. and Hutter J. L. (2009) Compositional and morphological features of aragonite precipitated experimentally from seawater and biogenically by corals. *Geochim. Cosmochim. Acta* **73**(14), 4166–4179.

Kakihana H., Kotaka M., Satoh S., Nomura M. and Okamoto M. (1977) Fundamental studies on the ion-exchange separation of boron isotopes. *Chem. Soc. Jpn.* **B50**, 158–163.

Kleypas J., Feely R., Fabry V. J., Langdon C., Sabine C. L. and Robbins L. (2006) *Impacts of Ocean Acidification on Coral Reefs and Other Marine Calcifiers: A Guide for Future Research*. NSF, NOAA, and USGS, St. Petersburg, FL, p. 88.

Klochko K., Kaufman A. J., Yoa W., Byrne R. H. and Tossell J. A. (2006) Experimental measurement of boron isotope fractionation in seawater. *Earth Planet. Sci. Lett.* **248**, 261–270.

Klochko K., Cody G. D., Tossell J. A., Dera P. and Kaufman A. J. (2009) Re-evaluating boron speciation in biogenic calcite and aragonite using 11B MAS NMR. *Geochim. Cosmochim. Acta* **73**(7), 1890–1900.

Langdon C. and Atkinson M. J. (2005) Effect of elevated pCO_2 on photosynthesis and calcification of corals and interactions with seasonal change in temperature/irradiance and nutrient enrichment. *J. Geophys. Res.* **110**(C09S07), 16.

Lewis E. and Wallace D. W. R. (1998) Program Developed for CO_2 System Calculations. In (C.D.I.A. Center). Oak Ridge National Laboratory, U.S. Department of Energy, ORNL/CDIAC-105, p. 21.

Lowenstam H. A. and Weiner S. (1989) *On Biomineralization*. Oxford University Press, New York, p. 336.

Maier C., Hegeman J., Weinbauer M. G. and Gattuso J. P. (2009) Calcification of the cold-water coral *Lophelia pertusa* under ambient and reduced pH. *Biogeosciences* **6**(8), 1671–1680.

Marion G. M., Millero F. J. B., Camões M. F., Spitzer P., Feistel R. and Chen C.-T. A. (2011) pH of seawater. *Mar. Chem.* **126**, 89–96.

Marubini F., Ferrier-Pagès C., Furla P. and Allemand D. (2008) Coral calcification responds to seawater acidification: a working hypothesis towards a physiological mechanism. *Coral Reefs* **27**, 491–499.

McCulloch M., Taviani M., Montagna P., López Correa M., Remia A. and Mortimer G. (2010) Proliferation and demise of Mediterranean deep-sea corals during the Younger Dryas. *Earth Planet. Sci. Lett.* **298**(1/2), 143–152.

Meibom A., Mostefaoui S., Cuif J. P., Dauphin Y., Houlbrèque F., Dunbar R. and Constantz B. (2007) Biological forcing controls the chemistry of reef-building coral skeleton. *Geophys. Res. Lett.* **34**(2), 5 (L02601).

Montagna P., McCulloch M., Taviani M., Mazzoli C. and Vendrell B. (2006) Phosphorous in cold-water corals as a proxy for seawater nutrient chemistry. *Science* **312**, 1788–1791.

Moya A., Tambutté S., Bertucci A., Tambutté E., Lotto S., Vullo D., Supuran C. T., Allemand D. and Zoccola D. (2008) Carbonic anhydrase in the scleractinian coral *Stylophora pistillata* characterization, localization, and role in biomineralization. *J. Biol. Chem.* **283**(37), 25475–25484.

Orr J. C., Fabry V. J., Aumont O., Bopp L., Doney S. C., Feely R. A., Gnanadesikan A., Gruber N., Ishida A., Joos F., Key R. M., Lindsay K., Maier-Reimer E., Matear R., Monfray P., Mouchet A., Najjar R. G., Plattner G.-K., Rodgers K. B.,

Sabine, Sarmiento J. L., Schlitzer R., Slater R. D., Totterdell I. J., Weirig M.-F., Yamanaka Y. and Yool A. (2001) Anthropogenic ocean acidification over the twenty-first century and its impact on calcifying organisms. *Nature* **437**, 681–686.

Pelejero C., Calvo E., McCulloch M. T., Marshall J. F., Gagan M. K., Lough J. M. and Opdyke B. N. (2005) Preindustrial to modern interdecadal variability in coral reef pH. *Science* **309**(5744), 2204–2207.

Rae J. W. B., Foster G. L., Schmidt D. N. and Elliott T. (2011) Boron isotopes and B/Ca in benthic foraminifera: proxies for the deep ocean carbonate system. *Earth Planet. Sci. Lett.* **302**, 403–413.

Ries J. B. (2011) A physicochemical framework for interpreting the biological calcification response to CO_2-induced ocean acidification. *Geochim. Cosmochim. Acta* **75**, 4053–4064.

Roberts J. M., Wheeler A. J. and Freiwald A. (2006) Reefs of the deep: the biology and geology of cold-water coral ecosystems. *Science* **312**(5773), 543–547.

Rollion-Bard C., Blamart D., Trebosc J., Tricot G., Mussi A. and Cuif J.-P. (2011) Boron isotopes as pH proxy: a new look at boron speciation in deep-sea corals using ^{11}B MAS NMR and EELS. *Geochim. Cosmochim. Acta* **75**, 1003–1012.

Rustad J. R., Bylaska E. J., Jackson V. E. and Dixon D. A. (2010) Calculation of boron-isotope fractionation between $B(OH)_{3(aq)}$ and $B(OH)^-_{4(aq)}$. *Geochim. Cosmochim. Acta* **74**, 2843–2850.

Sen S., Stebbins J. F., Hemming N. G. and Ghosh B. (1994) Coordination environments of B impurities in calcite and aragonite polymorphs: a ^{11}B MAS NMR study. *Am. Mineral.* **79**, 819–825.

Tambutté S., Tambutté E., Allemand D., Zoccola D., Meibom A., Lotto S. and Caminiti N. (2007) Observations of the tissue-skeleton interface in the scleractinian coral *Stylophora pistillata*. *Coral Reefs* **26**(3), 517–529.

Taviani M., Vertino A., López Correa M., Savini A., De Mol B., Remia A., Montagna P., Angeletti L., Zibrowius H., Alves T., Salomidi M., Ritt B. and Henry P. (2011) Pleistocene to recent deep-water corals and coral facies in the Eastern Mediterranean. *Facies* **57**(4), 579–603.

Thresher R. E., Tilbrook B., Fallon S., Wilson N. C. and Adkins J. (2011) Effects of chronic low carbonate saturation levels on the distribution, growth and skeletal chemistry of deep-sea corals and other seamount megabenthos. *Mar. Ecol. Prog. Ser.* **442**, 87–99.

Trotter J. A., Montagna P., McCulloch M. T., Silenzi S., Reynaud S., Mortimer G., Martin S., Ferrier-Pagès C., Gattuso J.-P. and Rodolfo-Metalpa R. (2011) Quantifying the pH 'vital effect' in the temperate zooxanthellate coral *Cladocora caespitosa*: validation of the boron seawater pH proxy. *Earth Planet. Sci. Lett.* **303**, 163–173.

Turley C. M., Roberts J. M. and Guinotte J. M. (2007) Corals in deep-water: will the unseen hand of ocean acidification destroy cold-water ecosystems? *Coral Reefs* **26**, 445–448.

Vengosh A., Chivas A. R. and McCulloch M. T. (1989) Direct determination of boron and chlorine isotopic compositions in geological-materials by negative thermal-ionization mass-spectrometry. *Chem. Geol.* **79**(4), 333–343.

Vengosh A., Kolodny Y., Starinsky A., Chivas A. R. and McCulloch M. T. (1991) Coprecipitation and isotopic fractionation of boron in modern biogenic carbonates. *Geochim. Cosmochim. Acta* **55**(10), 2901–2910.

Venn A., Tambutté E., Holcomb M., Allemand D. and Tambutté S. (2011) Live tissue imaging shows reef corals elevate pH under their calcifying tissue relative to seawater. *PLoS One* **6**(5), e20013.

Walter L. M. and Morse J. W. (1985) The dissolution kinetics of shallow marine carbonates in seawater: a laboratory study. *Geochim. Cosmochim. Acta* **49**, 1503–1513.

Wei G., McCulloch M. T., Mortimer G., Deng W. and Xie L. (2009) Evidence for ocean acidification in the Great Barrier Reef of Australia. *Geochim. Cosmochim. Acta* **73**, 2332–2346.

Zeebe R. (2005) Stable boron isotope fractionation between dissolved B(OH)3 and $B(OH)^-_4$. *Geochim. Cosmochim. Acta* **69**, 2753–2766.

Zeebe R. and Wolf-Gladow D. A. (2001) *CO_2 in Seawater: Equilibrium, Kinetics, Isotopes*, vol. 65. Elsevier Oceanography Series, Elsevier, Amsterdam.

Associate editor: Anders Meibom